SSRG International Journal of Civil Engineering
ISSN: 2348-8352/ https://doi.org/10.14445/23488352/IJCE-V12I4P109

Volume 12 Issue 4, 87-99, April 2025

Original Article

Flood Risk Mapping for Tlawng River Basin in Mizoram

Sagar Debbarma[1*], Vithono Tase[1], Bhaskarjyoti Buragohain[2], Sanayanbi Hodam[2], Arnab Bandyopadhyay[1]

[1]*Department of Agricultural Engineering, NERIST, Nirjuli, Arunachal Pradesh, India.*
[2]*NERIWALM, Dolabari, Tezpur, Assam, India.*

[*]*Corresponding Author : sagarbd33@gmail.com*

Received: 06 February 2025 Revised: 08 March 2025 Accepted: 09 April 2025 Published: 30 April 2025

Abstract *- Floods are among the worst devastating catastrophes on earth, leading to substantial loss of life and harm to buildings and infrastructure. 1.47 billion individuals worldwide face the threat of flooding. The Northeastern region of India, including Mizoram, is particularly vulnerable due to its hilly terrain, fragile ecosystem, and heavy monsoon rainfall. The Tlawng River, the longest river in Mizoram (185 km within the state), experiences frequent flooding, with the most recent major flood in 2019 affecting 1,968 families across 205 villages. Despite the devastating impacts of floods in the region, a comprehensive flood risk assessment has not yet been carried out for the entire Tlawng River Basin. The present research integrates a GIS-based MCA with AHP to develop a flood risk assessment for the Tlawng River Basin. Flood hazard indicators, consisting of MNDWI, NDVI, distance to river, slope, drainage density, TWI, elevation, rainfall, and lithology, were analyzed alongside vulnerability indicators such as LULC, population density, and proximity to roads and hospitals. Spatial layers for each indicator were generated, and their relative weights were determined using pairwise comparisons in the AHP framework. The study generated a final flood risk map by integrating assessments of flood hazards and vulnerabilities. The findings show that high and very high flood-risk areas encompass approximately 41.6% (1,445.7 km²) of the study region.*

Keywords *- AHP, Flood hazard, Vulnerability, Risk, Tlawng river basin.*

1. Introduction

Water from sources like rivers, lakes, or oceans can overflow its normal boundaries, leading to flooding. This often occurs due to rising water levels or the failure of containment structures such as levees [1]. Flooding can occur due to factors like rapid snowmelt, heavy rain, severe winds above water, tsunamis, high waves, dams, levees, and other water-retaining construction failures.

Floods manifest in diverse forms, including urban floods, coastal floods, pluvial floods (ponding), flash floods, and riverine (fluvial) floods [2]. Among these, Flash floods are especially dangerous, as they can develop quickly with little warning, causing severe social, economic, and environmental harm [3].

Flooding has widespread impacts, frequently causing major economic losses, infrastructure damage, and social upheaval, as well as tragic loss of life [4]. Riverside communities are especially vulnerable to these catastrophic events. India is a major flood-prone country, responsible for 20% of global flood deaths [5]. The country gets around 75% of its yearly rainfall during the monsoon, worsening flood risks [6]. The Central Water Commission reports that 37 million hectares of farmland in India are at risk of flooding during this period [7]. Assessing flood risks is crucial to predict future floods and plan effective ways to reduce impacts. These efforts are important to lower the risks and improve readiness for areas susceptible to flooding.

Assessing flood risk considers the potential and likelihood impacts of flooding in a specific area [8]. This comprehensive approach investigates potential flood hazards within the region, which is crucial for designing effective solutions to mitigate and control the impacts of floods [9]. Several methodologies have been used to evaluate flood risk, each one providing unique insights and tools. For example, hydrologic and hydraulic models were combined with decision-making frameworks, like multi-attribute utility theory [10] and AHP, to evaluate flood-related damages [11]. Other approaches include Multi-criteria Analysis (MCA) [12], Principal Component Analysis [14], statistical models [13], Frequency Ratio, and Cluster Analysis. Indicator-based indexing [15] and advanced GIS modelling techniques have also proven useful in flood risk assessment [16]. GIS, hydraulic models, and DEM data were shown to be useful for mapping probable flood zones and depths [17]. Similarly, the Analytic Hierarchy Process gained importance in analysing complicated geographical scenarios [18]. AHP uses mathematical and psychological concepts to study decision-making [19]. AHP, developed by Thomas L. Saaty in 1980, is often used to measure flood risk [20]. It prioritizes hazard and vulnerability elements.

Tlawng River experiences significant flood threats because of its geographic location and climate [21]. Yet, comprehensive flood risk mapping throughout the basin is urgently required for effective flood management and mitigation. Recent research has begun to address this issue, but important gaps still exist. A flood risk assessment by Debbarma et al. (2024) focused only on the physical features of the watershed in two locations, Bairabi and Sairang, leaving the larger Tlawng River Basin insufficiently evaluated [22]. The study extends flood risk mapping by incorporating the entire Tlawng River Basin. It considers both hazard factors, which define the physical features of the watershed, and vulnerability parameters, which represent the susceptibility of the local population [23]. By incorporating various vulnerability and hazard indicators, the study gives an additional overview of flood threat in the region.

This research creates a comprehensive flood risk map for the entire Tlawng River Basin using a GIS-based MCA and AHP. The method involves assigning weights to hazard and vulnerability indicators [24]. AHP and GIS provide a logical and precise evaluation of flood risk, considering both socioeconomic and physical influences [25].

Flooding in the Tlawng River Basin threatens lives, ruins infrastructure, and hinders commercial activities; therefore, careful risk assessment is crucial to protect people and support regional growth [26]. Flood risk maps are critical for Mizoram's IWRD. It will help in evacuation planning, flood preparedness, and resource allocation, reducing the impacts of flooding in the region.

2. Materials and Methods

2.1. Research Area

Tlawng River is the longest river in Mizoram, covering 185 kilometers. It starts in Zopui Hills at 1600 meters above MSL, situated 9 km east of city Lunglei at 22°66'10.624"N and 92°50'1.59"E. The basin covers a large area of 3500 km^2 within five districts in Mizoram. Many tributaries feed the river, the most known of being Tut and Teirei. Teirei goes into the Tlawng, improving flow and contributing to the basin's hydrology. Tlawng flows into the Barak River at Katakhal, hitting the lowest elevation of 8 m. The river then takes many names when it flows through Assam's Cachar district, including Dhaleswari and Katakhal.

The watershed has a tropical humid environment with annual rainfall of 2450 mm. The monsoon season changes the basin's hydrology and promotes dense vegetation and ecosystems. The climate in the basin has an average temperature of 21°C. The basin's geology consists of sedimentary rocks like sandstone, siltstone, and shale. Monsoon floods are common in the region, so understanding their behavior is important for the area's ecology and economy.

2.2. Acquisition of Data

The study used GIS-based MCA and AHP to create thematic layers for flood risk mapping. It used information from various resources like maps, satellite images, and primary and secondary data. ArcGIS 10.8 was used to produce maps of the distance to the river, drainage density, elevation, slope, and land use/land cover (LULC). SRTM DEM was used for drainage density, elevation, topographic wetness index (TWI), and slope. Landsat-8 imagery from the Living Atlas website was used to get LULC, Modified Normalized Water Index (MNDWI) and Normalized Difference Vegetation Index (NDVI). Additionally, 21 years of rainfall (2000–2020) from DES-PPI, Govt. of Mizoram and demographic data from Census of India were acquired. The statistical handbook of Mizoram was used to calculate the distance to hospitals.

2.3. Methodology

The study applied a GIS-based MCA combined with AHP to evaluate and analyze flood hazards and vulnerabilities over the entire Tlawng Basin. The process is visually shown in Figure 2. Key processes include choosing appropriate hazard and vulnerability indicators, assigning weights using AHP by pairwise comparisons, and computing vulnerability and hazard indices. These indicators were then combined to create a final flood risk map. The approach incorporates geomorphological, hydro-climatic, and socioeconomic parameters, enabling effective flood risk zoning [27].

2.3.1. GIS-Based MCA Using AHP for Weighting Indicators

The study used a GIS-based MCA with AHP to evaluate flood risk across the Tlawng River basin [22]. AHP was utilized to evaluate the importance of different factors through pairwise comparisons [28]. Each element was weighted based on its impact on hazards and vulnerability, giving a systematic and comprehensive analysis [29].

Selecting Indicators

The indicators were selected by considering their significance to flood risk and ability to capture hazard and vulnerability aspects [9]. Physical characteristics such as drainage density, slope, elevation, TWI, distance to the river, rainfall, and lithology were selected to evaluate flood hazards, as they directly influence water flow and flooding [30, 31]. Slope and elevation determine water flow and accumulation, while drainage density shows the basin's ability to drain excess water [32]. Distance to rivers shows nearness to flood-prone areas. Rainfall accounts for how climate affects flood frequency and intensity [33]. Lithology provides details on soil's ability to absorb and retain water [34].

On the other side, Socio-economic indicators, including LULC, distance to hospitals, proximity to roads, population density, and total population, were selected to measure flood vulnerability [35]. It shows the coverage, susceptibility, and resilience of communities to flooding. Total population and density indicate the amount of people in flood-prone areas

[31]. LULC alters runoff and infiltration [36]. Distance to hospitals and roads reflects access to emergency services and evacuation routes during emergencies [37]. This method gives a broad understanding of flood risk by considering both natural (hazard) and human (vulnerability) variables [38].

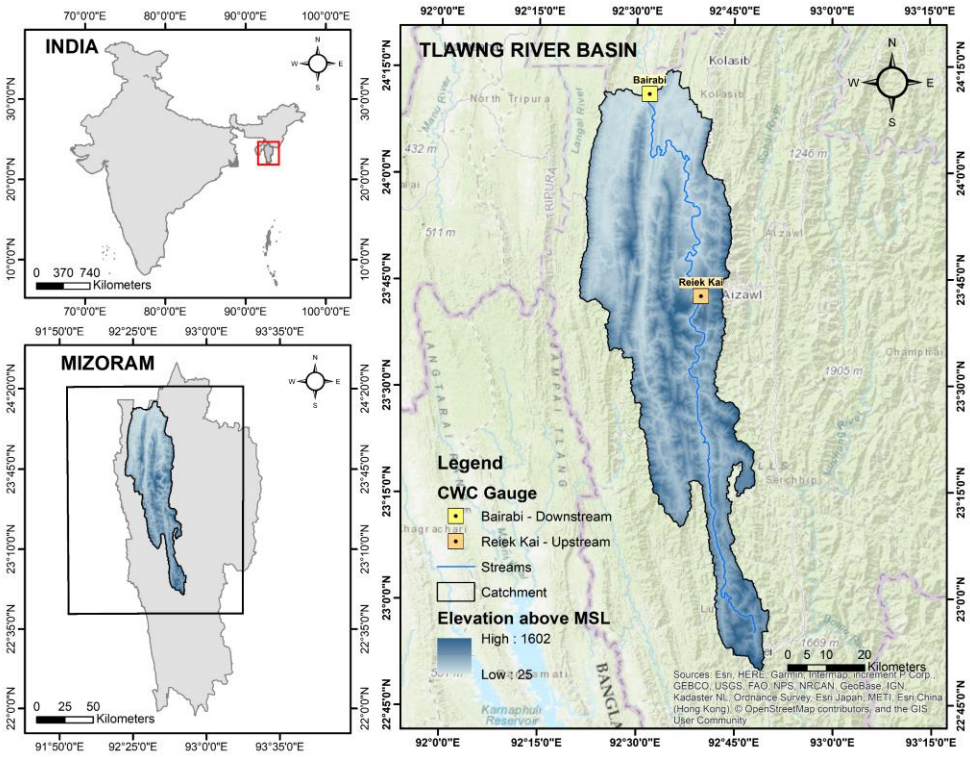

Fig. 1 Study area

AHP Weighting Process

AHP assigns weights to indicators by pairwise comparisons utilizing Saaty's scale preference between 1 and 9 [39]. Lower values indicate less importance and higher values signify greater importance [40]. Values in each row of the comparison matrix were multiplied, and the nth root of this product was then determined:

$$V_p = \sqrt[n]{W_1 \times \ldots\ldots \times W_n} \quad (1)$$

Where, V_p represents the eigenvector, W_n represents each element, and n represents total elements number (decision indicators).

The eigenvectors were normalized to derive weighting factors for each indicator [41]. To verify the reliability of the weighting process, the consistency ratio of the pairwise comparison matrix was computed (CR):

$$CR = \frac{CI}{RI} \quad (2)$$

Where RI denotes the random index and CI consistency index. CI was computed as:

$$CI = \frac{\lambda_{max}}{n-1} \quad (3)$$

In the above, λ_{max} represents the largest eigenvalue. According to Saaty (1980), a consistency ratio value of 10% or less indicates consistent judgments, and a higher value requires re-evaluation of pairwise comparisons.

Hazard Index (HI)

Flood hazard refers to the probability of natural phenomena occurring with varying intensities, which can lead to inundation and damage in surrounding areas [42]. These hazards are primarily driven by hydro-climatic factors influencing water flow dynamics, such as rainfall, slope, soil type, and drainage density [43].

According to Gigović et al. (2017) and Hazarika et al. (2018), the hazard can be described as the likelihood of destructive natural events within a specific spatial and temporal framework [44, 45]. To quantify flood hazard in the study area, a hazard index was computed by integrating multiple geophysical indicators, each weighted based on its contribution to flood occurrences [46]. The hazard index (HI) was obtained by applying the following equation:

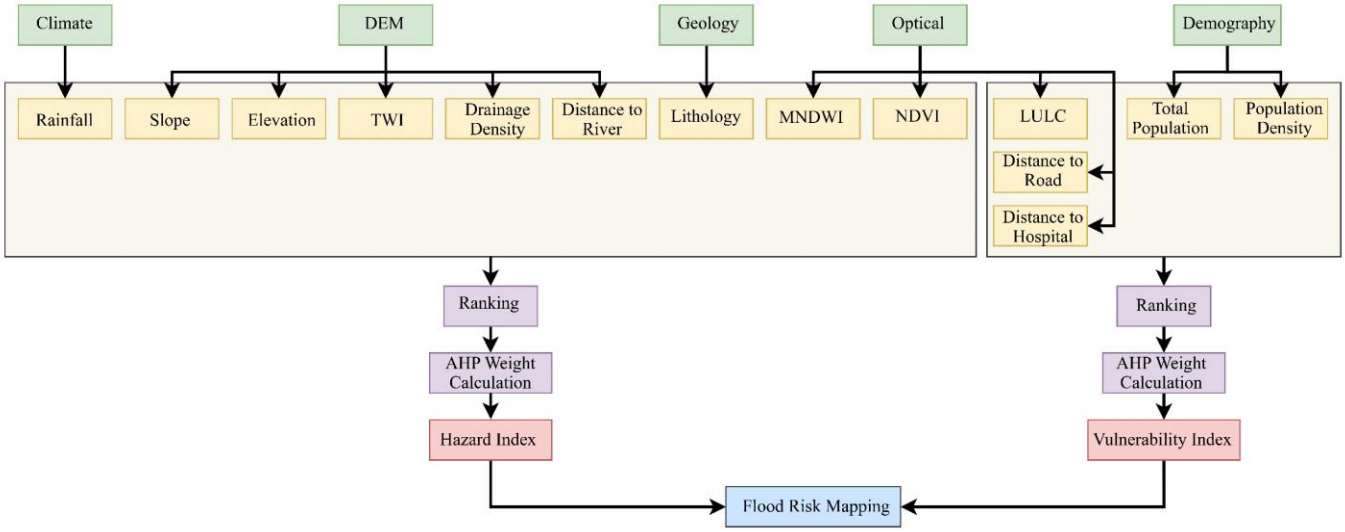

Fig. 2 Workflow for evaluating vulnerability, hazard, and flood risk in Tlawng River Basin

$$HI = W_E \times E + W_S \times S + W_{DD} \times DD + W_{DR} \times DR + W_{TWI} \times TWI + W_{MNDWI} \times MNDWI + W_R \times R + W_{NDVI} \times NDVI + W_L \times L \quad (4)$$

Where, S = slope; DR = distance to river; TWI = topographic wetness index; DD = drainage density; MNDWI = modified normalized difference water index; E = elevation; NDVI = normalized difference vegetative index; R = rainfall; L = Lithology.

Vulnerability Index (VI)

Flood vulnerability refers to how susceptible communities, infrastructure, and the environment are to flood-induced damage [47]. It includes exposure, susceptibility, and resilience, influenced by social, environmental, and economic factors [48]. Vulnerability changes over time due to land use, population, and economic trends [49]. It accounts for internal risks that can lead to losses in life, property, and resources [50]. The vulnerability index used socioeconomic indicators in this study to reflect community flood exposure. The vulnerability index (VI) was computed using a formula:

$$VI = W_{TP} \times TP + W_{PD} \times PD + W_{LULC} \times LULC + W_{DTH} \times DTH + W_{DTR} \times DTR \quad (5)$$

Where, TP = total population; LULC = land use land cover; DTR = distance to road; DTH = distance to hospital; PD = population density.

Flood Risk Index (FRI)

Flood risk represents the combined effects of flood vulnerability and hazard, indicating the potential for flood-induced damage in a region [51]. Flood risk mapping integrates hazard and vulnerability assessments to visualize flood-susceptible zones [52, 53]. In this research, flood risk was quantified by utilizing Flood Risk Index (FRI), computed as:

$$FRI = HI \times VI \quad (5)$$

Thematic layers representing hazard and vulnerability factors were weighted based on their importance and combined using a weighted sum approach. This approach helped identify and map flood-prone areas, supporting flood risk evaluation and prevention planning. The generated flood risk map is a key tool for emergency preparedness, infrastructure development, and policy development in the Tlawng River Basin.

3. Results

3.1. Results from Flood Hazard Mapping

Flood hazard refers to the likelihood of a flood occurrence of a given magnitude happening in a specific location and timeframe. A flood hazard map is essential for developing land use plans, particularly in flood potential regions. By generating comprehensive maps, this approach enables administrators and planners to recognize high-risk locations effectively and prioritize mitigation strategies accordingly. In this work, AHP was utilized to develop a pairwise comparison matrix (Table 1) based on expert judgment, assigning weights to each criterion leveraging Saaty's preference scale. The priority vector (V_p) was computed using Equation 1, followed by the normalization of the matrix (Table 2) by dividing each value in Table 1 by the total of its corresponding column. The maximum eigenvalue (λ_{max}) was determined as 9.93. With a random index (RI) value of 1.45, the computed CI and CR using Equations 2 and 3 were 0.12 and 0.08, respectively. The comparison matrix was considered consistent since the CR value (0.08) is below the acceptable threshold of 0.1. An analysis of the assigned weights revealed that elevation (0.20)

exerted the most significant influence on flood hazard, followed by slope (0.18), drainage density (0.16), and drainage relief (0.13). Other contributing factors included the TWI at 0.10, the MNDWI at 0.08, rainfall at 0.06, and both NDVI and land use at 0.05 (Table 3). Raster maps for these nine hazard parameters were prepared using ArcGIS 10.8, with individual parameter maps presented in Figure 3.

Table 1. Pairwise comparison matrix for hazard indicators

Variables	E	S	DD	DR	TWI	MNDWI	R	NDVI	L	V_p
E	1	3	2	2	3	2	3	2	2	2.12
S	1/3	1	3	4	2	2	3	2	3	1.88
DD	1/2	1/3	1	1	3	4	5	4	2	1.63
DR	1/2	1/4	1	1	3	2	3	2	4	1.38
TWI	1/3	1/2	1/3	1/3	1	3	4	3	3	1.08
MNDWI	1/2	1/2	1/4	1/2	1/3	1	3	2	2	0.79
R	1/3	1/3	1/5	1/3	1/4	1/3	1	3	2	0.54
NDVI	1/2	1/2	1/4	1/2	1/3	1/2	1/3	1	1	0.49
L	1/2	1/3	1/2	1/4	1/3	1/2	1/2	1	1	0.49
Total	4.50	6.75	8.53	9.92	13.25	15.33	22.83	20.00	20.00	10.40

Table 2. Normalized hazard matrix for multi-criteria flood risk assessment

Variables	E	S	DD	DR	TWI	MNDWI	R	NDVI	L	λ_{max}	CI	CR
E	0.24	0.57	0.28	0.26	0.33	0.14	0.15	0.08	0.08	9.93	0.12	0.08
S	0.08	0.19	0.42	0.52	0.22	0.14	0.15	0.08	0.12			
DD	0.12	0.06	0.14	0.13	0.33	0.28	0.25	0.16	0.08			
DR	0.12	0.05	0.14	0.13	0.33	0.14	0.15	0.08	0.16			
TWI	0.08	0.10	0.05	0.04	0.11	0.21	0.20	0.12	0.12			
MNDWI	0.12	0.10	0.04	0.07	0.04	0.07	0.15	0.08	0.08			
R	0.08	0.06	0.03	0.04	0.03	0.02	0.05	0.12	0.08			
NDVI	0.12	0.10	0.04	0.07	0.04	0.04	0.02	0.04	0.04			
L	0.12	0.06	0.07	0.03	0.04	0.04	0.03	0.04	0.04			

3.1.1. Flood Hazard Assessment and Classification

After determining the parameter weights, each layer was assigned its respective weight in ArcGIS 10.8. Using the weighted sum approach, hazard parameter values were divided into five groups: negligible (very low), minimal (low), intermediate (moderate), elevated (high), and extreme (very high). This category facilitated the establishment of a flood hazard susceptibility table, ranking parameters from 1 to 5 to represent increasing levels of susceptibility (Table 3). The final hazard map (Figure 4) was created through the weighted sum approach incorporating all nine parameters using Eq. 4. The resulting classification of the Tlawng River Basin into various flood hazard zones revealed that the majority of the basin falls within the moderate hazard class, followed by high and very low hazard categories. The extent for each hazard region is summarized in Table 4, highlighting that around 30.53% of the region is classified as moderate hazard, while 26.44% and 13.23% were categorized as high and very high hazard zones, respectively. The flood hazard mapping results underscore the critical role of topographic and hydrological parameters in flood susceptibility within the Tlawng River Basin. The integration of MCA and AHP provides a structured and objective assessment framework. The generated flood hazard map serves as an effective resource for managing flood risk, city development, and disaster preparedness in the region.

3.2. Results from Flood Vulnerability Mapping

Flood vulnerability parameters were ranked employing a pairwise comparison matrix, with each parameter assigned scores based on Saaty's preference scale as determined by expert opinion. The vulnerability parameter value (V_p) given in Eq. 1 has been calculated and is presented in Table 5. The normalization matrix was derived by dividing every single value in Table 8 by the total of its corresponding row.. The maximum Eigenvalue (λ_{max}) was found to be 5.27, with a random index (RI) value of 1.12 obtained from Table 3.

The CI and CR were calculated using Equations 2 and 3 and determined to be 0.07 and 0.06 (Table 6). Since the CR value (0.06) is below the acceptable threshold of 10%, the comparison matrix is deemed consistent (CR < 0.1). According to the AHP, the parameter weights were calculated with TP and PD exerting the strongest influence at 0.29, followed by LULC at 0.18, DTH at 0.14, and DTR at 0.10. Raster maps for these five indicators were generated using ArcGIS 10.8 software, as shown in Figure 5.

Table 3. Classification of flood hazard susceptibility

Parameters	Classes	Susceptible classes	Rank	Criteria weight
Elevation	25-241	N	1	0.20
	241-445	M	2	
	445-649	I	3	
	649-884	E	4	
	884-1602	EX	5	
Slope	0-10	N	1	0.18
	11-18	M	2	
	19-26	I	3	
	27-34	E	4	
	35-72	EX	5	
Drainage Density	0-30	N	1	0.15
	31-82	M	2	
	83-150	I	3	
	160-230	E	4	
	231-510	EX	5	
Distance to river	0-432	N	5	0.13
	433-999	M	4	
	1000-1490	I	3	
	1500-2060	E	2	
	2070-3800	EX	1	
TWI	-1-2	N	1	0.11
	3-6	M	2	
	7-9	I	3	
	10-15	E	4	
	16-20	EX	5	
MNDWI	-0.65-0.22	N	1	0.08
	-0.21- -0.17	M	2	
	-0.17- -0.13	I	3	
	-0.13- -0.076	E	4	
	-0.07-0.10	EX	5	
Rainfall	6-7	N	5	0.06
	7.1-7.4	M	4	
	7.5-7.8	I	3	
	7.9-8.6	E	2	
	8.7-9	EX	1	
NDVI	-0.06- 0.2	EX	5	0.05
	0.21- 0.28	E	4	
	0.29- 0.33	I	3	
	0.34- 0.39	M	2	
	0.4- 0.62	N	1	
Lithology	Clay	EX	5	0.05
	Mudstone	E	4	
	Sandstone	I	3	
	Shale	M	2	
	Siltstone	N	1	

*** N: Negligible; M: Minimal; I: Intermediate; E: Elevated; and EX: Extreme

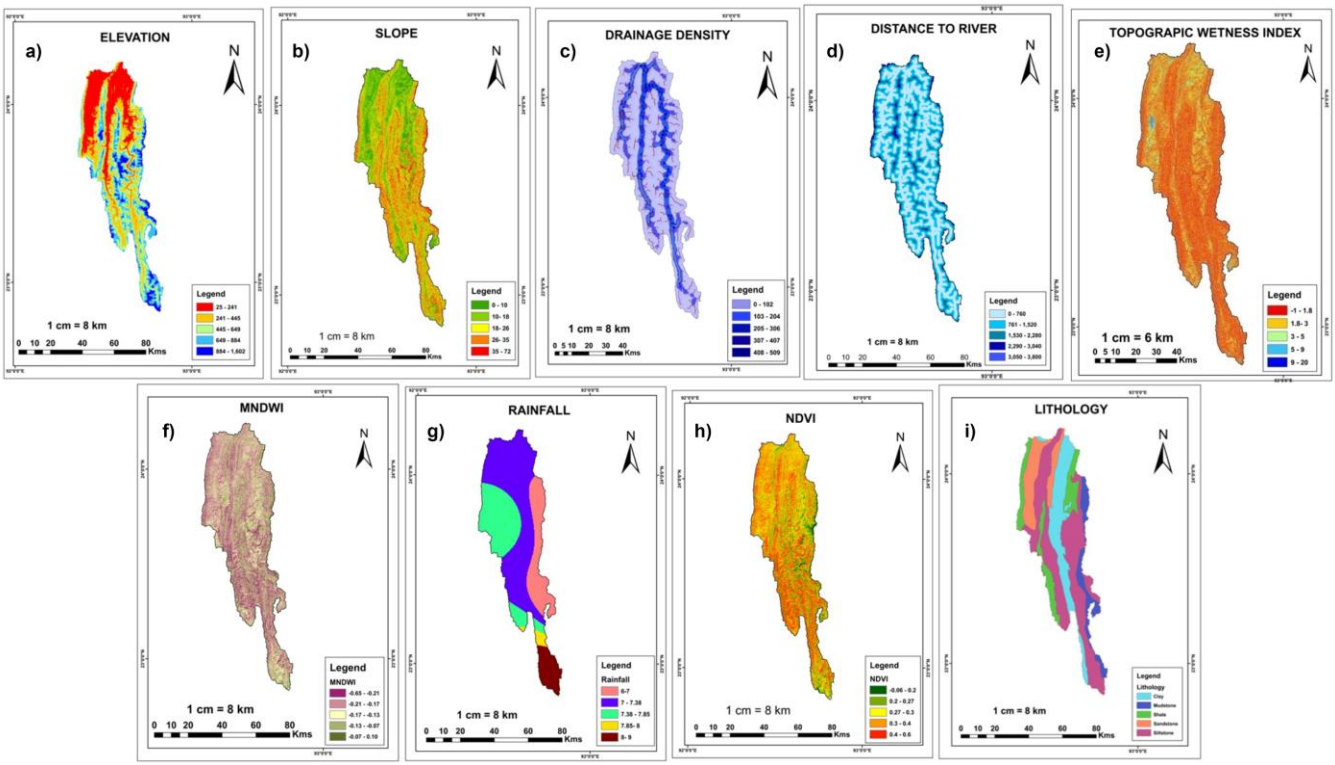

Fig. 3 Spatial distribution of flood hazard parameters: (a) Elevation, (b) Slope, (c) Drainage Density, (d) Distance to River, (e) TWI, (f) MNDWI, (g) Rainfall, (h) NDVI, and (i) Lithology.

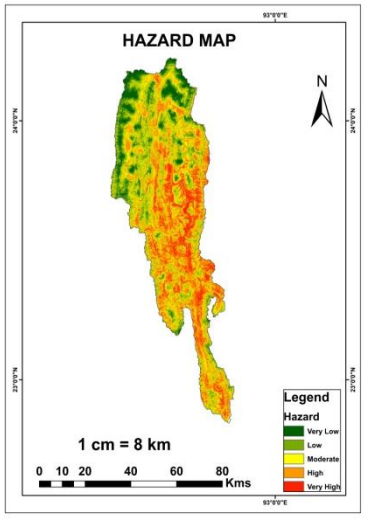

Fig. 4 Flood hazard mapping across the Tlawng River Basin

Table 4. Spatial extent of flood hazard areas

Hazard	Area (Km²)	Percentage (%)
Negligible	303.26	8.73
Minimal	732.33	21.07
Intermediate	1060.85	30.53
Elevated	918.70	26.44
Extreme	459.84	13.23
Total	3475.00	100.00

3.2.1. Pairwise Comparison and Normalized Matrices

Table 6 represents the pairwise comparison matrix of vulnerability indicators, demonstrating the relative influence of each parameter. Table 7 provides the normalized vulnerability matrix, which includes the computed values of λmax, CI, and CR.

3.2.2. Flood Vulnerability Classification

After determining the weights of each indicator, the layers were assigned corresponding weights in ArcGIS. The vulnerability parameter values were classified into five categories using the weighted sum approach: negligible, minimal, intermediate, elevated, and extreme.

A vulnerability susceptibility table was created to rank the parameters from 1 to 5, representing these levels of vulnerability (Table 8). The parameters were reclassified based on Table 7 and resampled to a resolution of 30 m.

The final flood vulnerability map was created by Eq. 5 in the weighted sum method. The comprehensive flood vulnerability map illustrates the geographic spread of flood susceptibility across the Tlawng River Basin, where different regions fall into varying vulnerability classes. The final vulnerability map is depicted in Figure 6, while Table 8 presents the corresponding area coverage of each flood vulnerability zone.

3.3. Results from Flood Risk Mapping

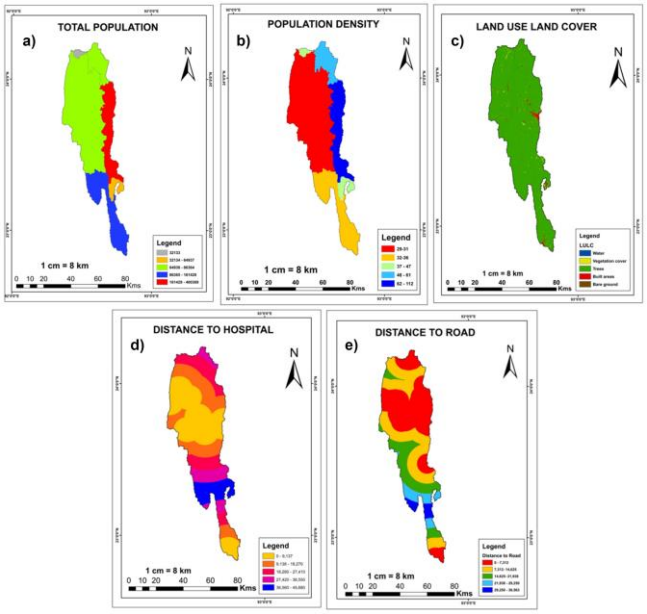

Fig. 5 Flood vulnerability parameters including (a) TP, (b) PD, (c) LULC, (d) DTH, and (e) DTR map.

Table 5. Pairwise comparison matrix for vulnerability indicators

Variables	TP	PD	LULC	DTH	DTR	V_p
TP	1	1	3	2	2	1.64
PD	1	1	3	2	2	1.64
LULC	1/3	1/3	1	2	3	0.92
DTH	1/2	1/2	1/2	1	2	0.76
DTR	1/2	1/2	1/3	1/2	1	0.53
Total	3.33	3.33	7.83	7.50	10.00	5.50

Table 6. Normalized vulnerability matrix for multi-criteria flood risk assessment

Variables	TP	PD	LULC	DTH	DTR	λ_{max}	CI	CR
TP	0.37	0.25	0.51	0.24	0.20	5.25	0.06	0.06
PD	0.37	0.25	0.51	0.24	0.20			
LULC	0.12	0.08	0.17	0.24	0.30			
DTH	0.19	0.13	0.09	0.12	0.20			
DTR	0.19	0.13	0.06	0.06	0.10			

The flood risk map of the research region is depicted in Figure 7, generated using Equation 6 in the raster calculator tool within ArcGIS 10.8. The analysis classified the flood risk into five distinct categories: negligible, minimal, intermediate, elevated, and extreme. These classifications were determined based on multiple flood-influencing factors, including topographic characteristics, hydrological parameters, and land use patterns. The flood risk map demonstrates that most of the research region is classified as moderate or high risk, suggesting the Tlawng River Basin is substantially vulnerable to flooding. Specifically, 27.95% (971.39 km²) of the area is categorized as moderate risk, while 27.61% (959.43 km²) falls under high-risk zones. The very high flood risk zone, covering 13.99% (486.27 km²), is primarily concentrated in regions with low elevations, floodplains, and regions with poor drainage. In contrast, areas with low and very low flood risk comprise 16.42% (570.53 km²) and 14.03% (487.38 km²) of the study region, respectively, mostly corresponding to elevated terrains and regions with efficient drainage. The detailed flood risk distribution is summarized in Table 9.

The findings indicate that nearly 70% of the research region was at moderate to very high risk of flooding, highlighting the urgency of looking for flood control strategies. Such high-risk zones are particularly significant for urban settlements, agricultural lands, and critical infrastructure located within the basin. The flood risk map becomes an essential tool for emergency preparedness, land-use strategy, and growth in infrastructure, enabling authorities to implement targeted flood control measures.

4. Discussion

The northeastern region of India frequently experiences extreme floods and landslides due to steep terrain and heavy monsoon rainfall. Mizoram is particularly vulnerable to flooding because of its rugged topography and intense seasonal precipitation, which leads to rapid runoff and river overflow. Despite the growing frequency and severity of floods, a comprehensive flood risk assessment has not been done for the entire Tlawng River Basin. This study uses a GIS-based multi-criteria approach with the Analytic Hierarchy Process to create a comprehensive flood risk mapping for the entire basin.

This research investigates the usage of GIS and AHP for flood risk evaluation in a mountainous watershed, where flooding is influenced by geomorphological and hydrological factors. Previous research by Darabi et al. (2019), Liu et al. (2021), and Karmakar et al. (2022) have applied these approaches in low-lying floodplains and urban areas [54-56], but this research demonstrates their effectiveness in a more complex, mountainous setting.

The study found that 41.6% of the area faces high to very high flood threat, highlighting the requirement for better flood prevention. The most influential hazards were topographic factors like elevation, slope, proximity to rivers, and drainage density. Vulnerability factors like population density, land use, and infrastructure access worsened flood risks in densely populated areas. Integrating these parameters provided a broader understanding of flood potential regions, improving the accuracy of risk mapping compared to single-factor analyses.

Table 7. Classification of flood vulnerability susceptibility

Parameters	Classes	Susceptibility class	Rank	Criteria weight
Total Population	86,365-118,140	EX	5	0.29
	118,150-145,740	E	4	
	145,750-178,350	I	3	
	178,360-225,180	M	2	
	225,190-299,600	N	1	
Population Density	29-40	EX	5	0.29
	41-49	E	4	
	50-57	I	3	
	58-69	M	2	
	70-90	N	1	
LULC	Bare ground	N	1	0.18
	Trees	M	2	
	Vegetation cover	I	3	
	Built areas	E	4	
	Water	EX	5	
Distance to hospital	0-8600	N	1	0.14
	8610-16,100	M	2	
	16,200-24,700	I	3	
	24,800-34,400	E	4	
	34,500-45,700	EX	5	
Distance to road	0-5018	N	1	0.10
	5019-10,470	M	2	
	10,480-16,490	I	3	
	16,500-24,380	E	4	
	24,390-36,560	EX	5	

4.1. Practical Implications and Limitations

The AHP approach provides a structured method for assigning weights to flood hazard and vulnerability indicators, but it has limitations. One primary concern is the subjectivity in the pairwise comparison process [20].

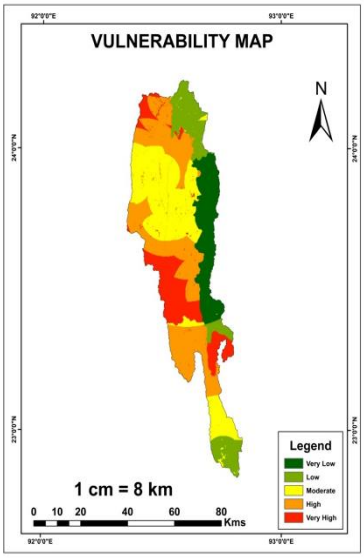

Fig. 6 Flood vulnerability mapping across the Tlawng River Basin

The weights depend on expert judgment, which can introduce bias and inconsistencies [57]. While the consistency ratio helps verify the logical coherence of the weights, human perception and expertise still influence the final weighting structure [58]. AHP assumes all decision criteria are independent, but complex interactions exist between hydrological, geomorphological, and socio-economic parameters that influence flood risk [59]. Additionally, as the number of indicators increases, the pairwise comparison process grows exponentially, making AHP more complex and time-consuming [60]. Despite these limitations, integrating AHP with GIS improves flood risk assessment by offering a clear and repeatable decision-making framework, especially in data-scarce areas like the Tlawng River Basin. Future studies could investigate blending AHP with machine learning or fuzzy logic to reduce subjectivity and enhance the robustness of flood risk assessments [61, 62].

Table 8. Spatial extent of flood vulnerability areas

Vulnerability	Area (Km²)	Percentage (%)
Negligible	494.16	14.10
Minimal	454.70	12.98
Intermediate	976.46	27.87
Elevated	1066.51	30.44
Extreme	511.95	14.61
Total	3503.78	100.00

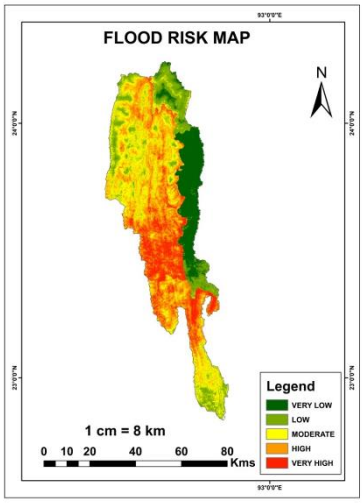

Fig. 7 Flood risk mapping across the Tlawng River Basin

Table 9. Spatial extent of flood risk areas

Flood Risk	Area (Km²)	Percentage (%)
Negligible	487.38	14.03
Minimal	570.53	16.42
Intermediate	971.39	27.95
Elevated	959.43	27.61
Extreme	486.27	13.99
Total	3475.00	100.00

5. Conclusion

The approach used for a multi-criteria approach to determine flood potential zones necessitated integrating both a hazard map (including factors such as NDVI, Rainfall, DTR, E, S, Lithology, TWI, DD, and MNDWI) and a vulnerability map (comprising DTH, LULC, PD, TP, and DTR). The generated map reveals an elevated risk of flooding in the lower sections of the basin, specifically in the Mamit, Lunglei, and Serchhip districts. The high-risk flooding area spans 1,445.7 km^2. Decision-makers can use this map to guide future preventive measures, improved land use planning, and flood risk management in the context of climate change. To conduct more detailed mapping in high-risk zones, it is essential to employ high-resolution satellite data, which will offer valuable insights and enhance the findings. Such studies can be performed at both district and basin levels, facilitating the development of more comprehensive risk maps and better-evaluating risks related to riverine flooding. Further research should incorporate high-resolution satellite data, machine learning, and hydrological models to enhance flood prediction and mapping accuracy.

Acknowledgements

The authors would like to acknowledge and sincerely thank the organizing committee of the International Conference on Computer-Aided Modeling for the Sustainable Development of Smart Cities (CAMSSC), sponsored by the Anusandhan National Research Foundation (ANRF), held at the Department of Civil Engineering, North Eastern Regional Institute of Science and Technology (NERIST), Nirjuli, Arunachal Pradesh, India, during November 27–30, 2024, for allowing us to present the paper and sponsoring the paper for publication.

Ethical Responsibilities of Authors

The authors have fulfilled their ethical responsibilities as researchers and acknowledge that, with minor exceptions, the list of authors cannot be altered once the paper has been submitted.

References

[1] Hasan Gul et al., "State-of-the-art Review on Stability and Serviceability of Dikes as a Flood Infrastructure and their Comprehensive Assessment in Indus Plain Considering Global Climate Change," *Natural Hazards*, vol. 120, pp. 13757-13809, 2024. [CrossRef] [Google Scholar] [Publisher Link]

[2] Iris Trikha, "*Urban Flooding Caused by Solid Waste: The Effect of Waste in Drainage Systems*," Master Thesis, University of Innsbruck, pp. 1-90, 2022. [Google Scholar] [Publisher Link]

[3] Duminda Perera et al., "Identifying Societal Challenges in Flood Early Warning Systems," *International Journal of Disaster Risk Reduction*, vol. 51, 2020. [CrossRef] [Google Scholar] [Publisher Link]

[4] Md. Ziaul Islam, and Chao Wang, "Cost of High-Level Flooding as a Consequence of Climate Change Driver?: A Case Study of China's Flood-Prone Regions," *Ecological Indicators*, vol. 160, pp. 1-18, 2024. [CrossRef] [Google Scholar] [Publisher Link]

[5] Manish Pandey et al., "Optimized Ensemble-based Flood Hazard Mapping in Low Altitude Subtropical Riverine Terrane," *Discover Geoscience*, vol. 2, pp. 1-32, 2024. [CrossRef] [Google Scholar] [Publisher Link]

[6] Ravinder Dhiman et al., "Flood Risk and Adaptation in Indian Coastal Cities: Recent Scenarios," *Applied Water Science*, vol. 9, pp. 1-16, 2019. [CrossRef] [Google Scholar] [Publisher Link]

[7] Ch. Srinivasarao et al., *Chapter Two - Agriculture Contingency Plans for Managing Weather Aberrations and Extreme Climatic Events: Development, Implementation and Impacts in India*, Advances in Agronomy, Academic Press, vol. 159, pp. 35-91, 2020. [CrossRef] [Google Scholar] [Publisher Link]

[8] Eoin O'Neill et al., "The Impact of Perceived Flood Exposure on Flood-Risk Perception: The Role of Distance," *Risk Analysis*, vol. 36, no. 11, pp. 2158-2186, 2016. [CrossRef] [Google Scholar] [Publisher Link]

[9] Sufia Rehman et al., "A Systematic Review on Approaches and Methods Used for Flood Vulnerability Assessment: Framework for Future Research," *Natural Hazards*, vol. 96, pp. 975-998, 2019. [CrossRef] [Google Scholar] [Publisher Link]

[10] Babak Zolghadr-Asli et al., "A Review of 20-Year Applications of Multi-Attribute Decision-Making in Environmental and Water Resources Planning and Management," vol. 23, pp. 14379-14404, 2021. [CrossRef] [Google Scholar] [Publisher Link]

[11] Jiquan Zhang et al., "Risk Assessment and Zoning of Flood Damage Caused by Heavy Rainfall in Yamaguchi Prefecture, Japan," *Proceedings of the 2nd Symposium on Flood Defence: Flood Defence*, Beijing, pp. 162-169, 2002. [Google Scholar] [Publisher Link]

[12] Yu Chen, "Flood Hazard Zone Mapping Incorporating Geographic Information System (GIS) and Multi-criteria Analysis (MCA) Techniques," *Journal of Hydrology*, vol. 612, 2022. [CrossRef] [Google Scholar] [Publisher Link]

[13] L. Collet, L. Beevers, and M. D. Stewart, "Decision-Making and Flood Risk Uncertainty: Statistical Data Set Analysis for Flood Risk Assessment," *Water Resources Research*, vol. 54, no. 10, pp. 7291-7308, 2018. [CrossRef] [Google Scholar] [Publisher Link]

[14] Tao Wu, "Quantifying Coastal Flood Vulnerability for Climate Adaptation Policy Using Principal Component Analysis," *Ecological Indicators*, vol. 129, pp. 1-12, 2021. [CrossRef] [Google Scholar] [Publisher Link]

[15] Won-joon Wang et al., "Flood Risk Assessment Using an Indicator Based Approach Combined with Flood Risk Maps and Grid Data," *Journal of Hydrology*, vol. 627, 2023. [CrossRef] [Google Scholar] [Publisher Link]

[16] Mahyat Shafapour Tehrany, Biswajeet Pradhan, and Mustafa Neamah Jebur, "Flood Susceptibility Mapping using a Novel Ensemble Weights-of-evidence and Support Vector Machine Models in GIS," *Journal of hydrology*, vol. 512, pp. 332-343, 2014. [CrossRef] [Google Scholar] [Publisher Link]

[17] A. J. Brimicombe, and J. M. Bartlett, "Linking Geographical Information Systems with Hydraulic Simulation Modeling for Flood Assessment: The Hong Kong Approach," *Second International Conference/Workshop on Integrating Geographic Information Systems and Environmental Modeling*, Breckenridge, Colorado, vol. 120, 1993. [Google Scholar]

[18] Singam Laxman Swamy et al., "Modeling Land-Degradation Vulnerability in Coal-Mined Environs through Geospatial and AHP Techniques: Potential Strategies for Eco-Restoration," *Environmental Science and Pollution Research*, 2024. [CrossRef] [Google Scholar] [Publisher Link]

[19] Tibor Krenicky, Liudmyla Hrebenyk and Vadym Chernobrovchenko, "Application of Concepts of the Analytic Hierarchy Process in Decision-Making," *Management Systems in Production Engineering*, vol. 30, no. 4, pp. 304-310, 2022. [CrossRef] [Google Scholar] [Publisher Link]

[20] Thomas L. Saaty, "How to Make a Decision: The Analytic Hierarchy Process," *European Journal of Operational Research*, vol. 48, no. 11, pp. 9-26, 1990. [CrossRef] [Google Scholar] [Publisher Link]

[21] Sagar Debbarma, Arnab Bandyopadhyay, and Aditi Bhadra, "Streamflow Simulation Using a Hybrid Approach Combining HEC-HMS and LSTM Model in the Tlawng River Basin of Mizoram, India," *Environmental Modeling & Assessment*, 2025. [CrossRef] [Google Scholar] [Publisher Link]

[22] Sagar Debbarma et al., "Optimum Flood Inundation Mapping in Mountainous Regions using Sentinel-1 Data and a GIS-based Multi-Criteria Approach: A Case Study of Tlawng River Basin, Mizoram, India," *Environmental Monitoring and Assessment*, vol. 196, 2024. [CrossRef] [Google Scholar] [Publisher Link]

[23] Shifa Chen et al., "Evaluation of Soil Erosion Vulnerability on the Basis of Exposure, Sensitivity, and Adaptive Capacity: A Case Study in the Zhuxi Watershed, Changting, Fujian Province, Southern China," *Catena*, vol. 177, pp. 57-69, 2019. [CrossRef] [Google Scholar] [Publisher Link]

[24] Niraj Kumar, and Ramakar Jha, "GIS-based Flood Risk Mapping: The Case Study of Kosi River Basin, Bihar, India," *Engineering, Technology & Applied Science Research*, vol. 13, no. 1, pp. 9830-9836, 2023. [CrossRef] [Google Scholar] [Publisher Link]

[25] Aptu Andy Kurniawan et al., "Flood Management on GIS-Based Multicriteria Evaluation in Developing Countries: A Systematic Literature Review," *Environmental and Earth Sciences*, pp. 1-23, 2024. [CrossRef] [Google Scholar] [Publisher Link]

[26] David A. Lalramchulloa, Udaya Bhaskra Rao, and P. Rinawma, "Morphometric and Sinuosity Analysis of Tlawng River Basin: A Geographic Information System Approach," *Journal of Geographical Studies*, vol. 5, no. 1, pp. 22-32, 2021. [CrossRef] [Google Scholar] [Publisher Link]

[27] Aastha Sharma et al., "A Systematic Review for Assessing the Impact of Climate Change on Landslides: Research Gaps and Directions for Future Research," *Spatial Information Research*, vol. 32, pp. 165-185, 2024. [CrossRef] [Google Scholar] [Publisher Link]

[28] Gang Kou et al., "Pairwise Comparison Matrix in Multiple Criteria Decision Making," *Technological and Economic Development of Economy*, vol. 22, no. 5, pp. 738-765, 2016. [CrossRef] [Google Scholar] [Publisher Link]

[29] Jeetendra Sahani et al., "Hydro-Meteorological Risk Assessment Methods and Management by Nature-based Solutions," *Science of the Total Environment*, vol. 696, pp. 1-17, 2019. [CrossRef] [Google Scholar] [Publisher Link]

[30] J. C. J. H. Aerts et al., "Integrating Human Behaviour Dynamics into Flood Disaster Risk Assessment," *Nature Climate Change*, vol. 8, pp. 193-199, 2018. [CrossRef] [Google Scholar] [Publisher Link]

[31] Mohamed Zhran et al., "Exploring a GIS-based Analytic Hierarchy Process for Spatial Flood Risk Assessment in Egypt: A Case Study of the Damietta Branch," *Environmental Sciences Europe*, vol. 36, pp. 1-25, 2024. [CrossRef] [Google Scholar] [Publisher Link]

[32] David R. Montgomery, and John M. Buffington, "Channel-Reach Morphology in Mountain Drainage Basins," *Geological Society of America Bulletin*, vol. 109, no. 5, pp. 596-611, 1997. [CrossRef] [Google Scholar] [Publisher Link]

[33] Dejene Tesema Bulti, Birhanu Girma Abebe, and Zelalem Biru, "Climate Change–Induced variations in Future Extreme Precipitation Intensity–Duration–Frequency in Flood-Prone City of Adama, Central Ethiopia," *Environmental Monitoring and Assessment*, vol. 193, 2021. [CrossRef] [Google Scholar] [Publisher Link]

[34] Dacheng Xiao et al., "Streamflow Generation from Catchments of Contrasting Lithologies: The Role of Soil Properties, Topography, and Catchment Size," *Water Resources Research*, vol. 55, no. 11, pp. 9234-9257, 2019. [CrossRef] [Google Scholar] [Publisher Link]

[35] A.G. Palacio-Aponte, A.J. Ortíz-Rodríguez, and S. Sandoval-Solis, "Methodological Framework for Territorial Planning of Urban Areas: Analysis of Socio-Economic Vulnerability and Risk Associated with Flash Flood Hazards," *Applied Geography*, vol. 149, 2022. [CrossRef] [Google Scholar] [Publisher Link]

[36] Junjie Tang et al., "Impacts of Land Use Change on Surface Infiltration Capacity and Urban Flood Risk in a Representative Karst Mountain City Over The Last Two Decades," *Journal of Cleaner Production*, vol. 454, 2024 . [CrossRef] [Google Scholar] [Publisher Link]

[37] Marta Borowska-Stefańska et al., "Optimisation Patterns for the Process of a Planned Evacuation in the Event of a Flood," *Environmental Hazards*, vol. 18, no. 4, pp. 335-360, 2019. [CrossRef] [Google Scholar] [Publisher Link]

[38] Mohammad Aminur Rahman Shah et al., "A Review of Hydro-Meteorological Hazard, Vulnerability, and Risk Assessment Frameworks and Indicators in the Context of Nature-based Solutions," *International Journal of Disaster Risk Reduction*, vol. 50, pp. 1-12, 2020. [CrossRef] [Google Scholar] [Publisher Link]

[39] Francesca Abastante et al., "A New Parsimonious AHP Methodology: Assigning Priorities to Many Objects by Comparing Pairwise few Reference Objects, *Expert Systems with Applications*, vol. 127, pp. 109-120, 2019. [CrossRef] [Google Scholar] [Publisher Link]

[40] R. K. Jaiswal et al., "Watershed Prioritization Using Saaty's AHP Based Decision Support for Soil Conservation Measures," *Water Resources Management*, vol. 28, pp. 475-494, 2014. [CrossRef] [Google Scholar] [Publisher Link]

[41] Li Xu et al., "A Novel Decision-Making System for Selecting Offshore Wind Turbines with PCA and D Numbers," *Energy*, vol. 258, 2022. [CrossRef] [Google Scholar] [Publisher Link]

[42] Rofiat Bunmi Mudashiru et al., "Flood Hazard Mapping Methods: A Review," *Journal of Hydrology*, vol. 603, 2021. [CrossRef] [Google Scholar] [Publisher Link]

[43] Gowhar Meraj et al., "Assessing the Influence of Watershed Characteristics on the Flood Vulnerability of Jhelum Basin in Kashmir Himalaya," *Natural Hazards*, vol. 77, pp. 153-175, 2015. [CrossRef] [Google Scholar] [Publisher Link]

[44] Ljubomir Gigovic et al., "Application of GIS-Interval Rough AHP Methodology for Flood Hazard Mapping in Urban Areas," *Water*, vol. 9, no. 6, pp. 1-26, 2017. [CrossRef] [Google Scholar] [Publisher Link]

[45] N. Hazarika et al., "Assessing and Mapping Flood Hazard, Vulnerability and Risk in the Upper Brahmaputra River Valley Using Stakeholders' Knowledge and Multicriteria Evaluation (MCE)," *Journal of Flood Risk Management*, vol. 11, no. 2, S700-S716, 2018. [CrossRef] [Google Scholar] [Publisher Link]

[46] Cassie Roopnarine, Bheshem Ramlal, and Ronald Roopnarine, "A Comparative Analysis of Weighting Methods in Geospatial Flood Risk Assessment: A Trinidad Case Study," *Land*, vol. 11, no. 10, pp. 1-30, 2022. [CrossRef] [Google Scholar] [Publisher Link]

[47] Md Nazirul Islam Sarker et al., "Assessment of Flood Vulnerability of Riverine Island Community Using a Composite Flood Vulnerability Index," *International Journal of Disaster Risk Reduction*, vol. 82, 2022. [CrossRef] [Google Scholar] [Publisher Link]

[48] S. F. Balica, N. G. Wright, and F. van Der Meulen, "A Flood Vulnerability Index for Coastal Cities and its Use in Assessing Climate Change Impacts," *Natural Hazards*, vol. 64, pp. 73-105, 2012. [CrossRef] [Google Scholar] [Publisher Link]

[49] Juan Carlos Villagran De Leon, *Vulnerability A Conceptual and Methodological Review*, United Nations University Institute for Environment and Human Security, pp. 1-64, 2006. [Google Scholar] [Publisher Link]

[50] Abhishek Ghosh, and Shyamal Kumar Kar, "Application of Analytical Hierarchy Process (AHP) for Flood Risk Assessment: A Case Study in Malda District of West Bengal, India," *Natural Hazards*, vol. 94, pp. 349-368, 2018. [CrossRef] [Google Scholar] [Publisher Link]

[51] Dev Anand Thakur, and Mohit Prakash Mohanty, "A Synergistic Approach towards Understanding Flood Risks Over Coastal Multi-Hazard Environments: Appraisal of Bivariate Flood Risk Mapping through Flood Hazard, and Socio-Economic-Cum-Physical Vulnerability Dimensions," *Science of the Total Environment*, vol. 901, 2023. [CrossRef] [Google Scholar] [Publisher Link]

[52] Yashon O. Ouma, and Ryutaro Tateishi, "Urban Flood Vulnerability and Risk Mapping Using Integrated Multi-Parametric AHP and GIS: Methodological Overview and Case Study Assessment," *Water*, vol. 6, no. 6, pp. 1515-1545, 2014. [CrossRef] [Google Scholar] [Publisher Link]

[53] Mohamed Mohamed Yagoub, "Spatio-Temporal and Hazard Mapping of Earthquake in UAE (1984–2012): Remote Sensing and GIS Application," *Geoenvironmental Disasters*, vol. 2, pp. 1-14, 2015. [CrossRef] [Google Scholar] [Publisher Link]

[54] Hamid Darabi et al., "Urban Flood Risk Mapping Using the GARP and Quest Models: A Comparative Study of Machine Learning Techniques," *Journal of Hydrology*, vol. 569, pp. 142-154, 2019. [CrossRef] [Google Scholar] [Publisher Link]

[55] Wen-Cheng Liu, Tien-Hsiang Hsieh, and Hong-Ming Liu, "Flood Risk Assessment in Urban Areas of Southern Taiwan," *Sustainability*, vol. 13, no. 6, pp. 1-22, 2021. [CrossRef] [Google Scholar] [Publisher Link]

[56] Subhankar Karmakar, M. A. Sherly, and Mohit Mohanty, *Urban Flood Risk Mapping: A State-of-the-Art Review on Quantification, Current Practices, and Future Challenges*, Advances in Urban Design and Engineering: Perspectives from India, Springer, pp. 125-156, 2022. [CrossRef] [Google Scholar] [Publisher Link]

[57] Jakub Więckowski, Jarosław Wątróbski, and Wojciech Sałabun, "Inaccuracies in Expert Judgment: Comparative Analysis of RANCOM and AHP Methods in Housing Location Selection Problem," *IEEE Access*, vol. 12, pp. 142083-142100, 2024. [CrossRef] [Google Scholar] [Publisher Link]

[58] Haton E. Alhamad, and Saud M. Al-Mandil, "From Intuition to Optimization: A Hybrid FAHP-MAUT Model for Informed R&D Investment Decision in Mining," *Mining, Metallurgy & Exploration*, vol. 41, pp. 2457-2478. [CrossRef] [Google Scholar] [Publisher Link]

[59] Muluneh Legesse Edamo et al., "A Comparative Assessment of Multi-Criteria Decision-Making Analysis and Machine Learning Methods for Flood Susceptibility Mapping and Socio-Economic Impacts on Flood Risk in Abela-Abaya Floodplain of Ethiopia," *Environmental Challenges*, vol. 9, pp. 1-16, 2022. [CrossRef] [Google Scholar] [Publisher Link]

[60] Pijush Kanti Dutta Pramanik et al., "A Comparative Analysis of Multi-Criteria Decision-Making Methods for Resource Selection in Mobile Crowd Computing," *Symmetry*, vol. 13, no. 9, pp. 1-51, 2021. [CrossRef] [Google Scholar] [Publisher Link]

[61] Pranab Dutta, and Sujit Deka, "A Novel Approach to Flood Risk Assessment: Synergizing with Geospatial Based Mcdm-Ahp Model, Multicollinearity, and Sensitivity Analysis in the Lower Brahmaputra Floodplain, Assam," *Journal of Cleaner Production*, vol. 467, 2024. [CrossRef] [Google Scholar] [Publisher Link]

[62] Mohammad Syamsyul Hairi Saad et al., "A Preliminary Study on the Fuzzy Analytical Hierarchy Process (FAHP) for the Prioritization of Flash Flood Risk Index in Development Projects," *IOP Conference Series: Earth and Environmental Science: World Sustainable Construction Conference*, Kuala Lumpur, Malaysia, vol. 1444, pp. 1-23, 2025. [CrossRef] [Google Scholar] [Publisher Link]